Myeloid heme oxygenase–1 regulates innate immunity and autoimmunity by modulating IFN-β production

Sotiria Tzima, Panayiotis Victoratos, Ksanthi Kranidioti, Maria Alexiou, and George Kollias

Biomedical Sciences Research Center "Alexander Fleming," Vari 166-72, Greece

Heme oxygenase–1 (HO-1) is a key cytoprotective, antioxidant, and antiinflammatory molecule. The pathophysiological functions of HO-1 have been associated with its enzymatic activities in heme catabolism. We have examined the immune functions of HO-1 by its conditional ablation in myeloid cells (HO-1^{M-KO} mice). We demonstrate that myeloid HO-1 is required for the activation of interferon (IFN) regulatory factor (IRF) 3 after Toll-like receptor 3 or 4 stimulation, or viral infection. HO-1–deficient macrophages show reduced expression of IFN-β and of primary IRF3 target genes encoding RANTES, IP-10 and MCP-1. In the presence of polyI:C, myeloid HO-1 knockout mice infected with *Listeria monocytogenes*, a model dependent on IFN-β production, showed enhanced bacterial clearance and survival, whereas control mice succumbed to infection. Moreover, after induction of experimental autoimmune encephalomyelitis, mice with myeloid-specific HO-1 deficiency developed a higher incidence and an exacerbated, nonremitting clinical disease correlating with persistent activation of antigen-presenting cells, enhanced infiltration of Th17 cells, and a nonregressing myelin-specific T cell reactivity. Notably, these defects were rectified by exogenous administration of IFN-β, confirming that HO-1 functions directly upstream of this critical immune pathway. These results uncover a novel direct function for myeloid HO-1 in the regulation of IFN-β production, establishing HO-1 as a critical early mediator of the innate immune response.

CORRESPONDENCE
George Kollias:
kollias@fleming.gr

Abbreviations used: AP-1, adaptor protein 1; BMDM, BM macrophage; CNS, central nervous system; EAE, experimental autoimmune encephalomyelitis; GST, glutathione S-transferase; HO-1, heme oxygenase–1; IRF, IFN regulatory factor; ISRE, IFN-stimulated response element; LFB, luxol fast blue; MAPK, mitogen-activated protein kinase; MDA5, melanoma differentiation–associated gene 5; MOG, myelin oligodendrocyte glycoprotein; MOI, multiplicity of infection; PKR, protein kinase regulated by RNA; RIG-I, retinoic acid–inducible gene I; SeV, Sendai virus; TEPM, thioglycollate-elicited peritoneal macrophage; TIR, TLR–IL-1R; TLR, Toll-like receptor; TRIF, TIR domain–containing adaptor inducing IFN-β; WCE, whole-cell extract.

Recent advances have provided a clearer picture of the pathways by which the innate immune system senses bacterial and viral pathogens, and how this leads to the production of type I IFNs. This process is primarily mediated by the engagement of specific Toll-like receptors (TLRs) but also by TLR-independent pathways. The specific ligands recognized by IFN-α/β–inducing TLRs include dsRNA for TLR3 (1), LPS for TLR4 (2), ssRNA for TLR7 and 8 (3, 4), and unmethylated CpG-DNA for TLR9 (5). Ligand binding leads to TLR dimerization and conformational changes in both the receptor ectodomains and the cytoplasmic TLR–IL-1R (TIR) domains. TIR domains bind specific adaptors: TIR domain–containing adaptor inducing IFN-β (TRIF) for TLR3; TRIF-related adaptor molecule, TRIF, TIR domain–containing adaptor protein, and MyD88 for TLR4; and MyD88 for TLR7, 8, and 9 (6, 7). These adaptors propagate signaling by recruiting kinases that mediate activation of the transcription factors adaptor protein 1 (AP-1; heterodimer of activating transcription factor 2 and c-Jun), NF-κB, IFN regulatory factor (IRF) 3, and IRF7, which are all required for IFN-α/β production. Two cytosolic RNA helicases, retinoic acid–inducible gene I (RIG-I) and melanoma differentiation–associated gene 5 (MDA5), mediate TLR-independent IFN-α/β induction by actively replicating RNA viruses and synthetic RNA (8). RIG-I and MDA5 bind through caspase recruitment domains to mitochondrial IFN-β promoter stimulator 1 (9), initiating signaling cascades that lead to IRF3, IRF7, NF-kB, and AP-1 activation, and IFN-α/β expression. In addition to viral cytosolic RNA, bacterial cytosolic DNA also triggers TLR-independent type I IFN production

The Rockefeller University Press $30.00
J. Exp. Med. Vol. 206 No. 5 1167-1179
www.jem.org/cgi/doi/10.1084/jem.20081582

The Journal of Experimental Medicine

through an as yet not fully defined pathway that requires IRF3, but not activation of NF-κB and mitogen-activated protein kinases (MAPKs).

Heme oxygenase–1 (HO-1) is a key cytoprotective, antioxidant, and antiinflammatory molecule. Most of the physiological functions of HO-1 have been associated with its enzymatic activity in heme catabolism (10, 11). In humans, HO-1 deficiency is associated with susceptibility to oxidative stress and an increased proinflammatory state with severe endothelial damage (12). Mice lacking HO-1 develop progressive inflammatory disease (13) and show enhanced sensitivity to LPS-induced toxemia (14). The protective properties of HO-1 have been studied in a variety of inflammatory models (15–20); however, the molecular mechanisms, timing, and mode of HO-1 function in disease remain largely unknown.

Earlier studies have shown that HO-1 expression or CO administration mediate potent antiinflammatory effects in monocytes and/or macrophages (16, 17), probably restraining these cells from inducing tissue injury and possibly modulating their role in the initiation of immune responses. However, little is known about the signaling pathways that are regulated by HO-1 in macrophages, a cell type central to the initiation of immune and autoimmune responses. In this study, we sought to examine the function of HO-1 in immune responses by conditional ablation of HO-1 gene expression, specifically in macrophages. We demonstrate that HO-1 is not essential for TLR4/MyD88-induced NF-κB and MAPK activation and subsequent proinflammatory cytokine production, but is required for TLR4/TLR3/IRF3-induced production of IFN-β and primary IRF3 target genes in macrophages. In addition, IRF3 activation and subsequent IFN-β production was severely impaired in HO-1 knockout macrophages infected with Sendai virus (SeV). In the presence of polyI:C, myeloid HO-1 knockout mice infected with *Listeria monocytogenes*, an infectious model with enhanced severity that is dependent on IFN-β production, showed enhanced bacterial clearance, whereas control mice succumbed to infection. Furthermore, myeloid HO-1 deficiency exacerbated experimental autoimmune encephalomyelitis (EAE) in mice that was associated with defective IFN-β production and enhanced infiltration of activated macrophages and Th17 cells in the central nervous system (CNS).

RESULTS

Ubiquitous and myeloid-specific inactivation of HO-1 in mice

To investigate the function of HO-1 in immune responses, we generated mice with conditional deletion of the *Hmox1* allele (Fig. 1 A). To generate mice with ubiquitous deletion of the *Hmox1* gene ($Hmox1^{D/D}$ or HO-1^{KO} mice), we crossed $Hmox1^{FL/FL}$ mice with transgenic mice expressing Cre in germ cells (21). We confirmed deletion of *Hmox1* in the germline by Southern blot analysis (Fig. 1 B). Of ∼622 newborn pups obtained by intercrossing $Hmox1^{+/D}$ mice, we obtained 25 $Hmox^{D/D}$ mice, indicating, as previously described (13), that the HO-1 deficiency is partially embryonic lethal. HO-1^{KO} mice showed a progressive chronic inflammatory disease characterized by enlarged spleens and hepatic inflammatory lesions (Fig. 1 C), and died within 6 mo because of presumed multiorgan failure. Immunoblot analysis of thioglycollate-elicited peritoneal macrophage (TEPM) extracts from HO-1^{KO} mice showed complete ablation of HO-1 at the protein level (Fig. 1 D).

For myeloid-restricted ablation of HO-1, we crossed $Hmox1^{FL/FL}$ mice with *LysM*-Cre knockin mice. The *LysM*-Cre transgene mediates excision of *lox*P-flanked sequences in macrophages and granulocytes (22). Immunoblot analysis of TEPM extracts from $LysM^{Cre/+}Hmox1^{FL/FL}$ and $LysM^{Cre/+}Hmox1^{D/FL}$ mice demonstrated efficient ablation of HO-1 at the protein level as compared with TEPM extracts from $Hmox1^{FL/FL}$ or $Hmox1^{+/+}$ mice (Fig. 1 D). Mice with myeloid-restricted HO-1 deficiency were born at the expected Mendelian ratio, were viable and fertile, and did not show apparent abnormalities. Histological analysis of organ sections from these mice did not demonstrate any gross morphological defects (unpublished data).

HO-1 is not required for NF-κB and MAPK activation in response to TLR4 and TLR3 stimulation

To investigate innate immune defects in the absence of myeloid HO-1, peritoneal macrophages from $LysM^{Cre/+}Hmox1^{FL/FL}$ (HO-$1^{M\text{-}KO}$) and $Hmox1^{FL/FL}$ (control) mice were stimulated in vitro with LPS or polyI:C, and phosphorylation of the NF-κB and MAPKs was examined. Activation of IKK1, IKK2, IκB, ERK1/2, JNK2, and p38 occurred to the same extent and with similar kinetics in control and HO-$1^{M\text{-}KO}$ macrophages in response to LPS (Fig. S1 A) or polyI:C (Fig. S1 B). Moreover, no significant differences were observed in the production of TNF or IL-6 between control and HO-$1^{M\text{-}KO}$ macrophages or BM macrophages (BMDMs) from HO-1^{KO} mice in response to LPS or polyI:C (Fig. S1, C–E). Collectively, these results suggest that HO-1 is not required for TLR3- and TLR4-mediated activation of the NF-κB or AP-1 pathways in macrophages.

HO-1 deficiency impairs IFN-β production induced by TLR4 or TLR3 and is required for the induction of primary IRF3 target genes in macrophages

TLR3 and TLR4 signals induce gene transcription through DNA motifs, designated IFN-stimulated response elements (ISREs), found in promoters of genes that bind the IRF family of transcription factors (23, 24). These include early inflammatory genes, antiviral cytokines, and chemokines (25). We therefore examined whether HO-1 is required for the induction of these genes in response to dsRNA or LPS. After being stimulated with polyI:C, HO-1–deficient macrophages showed significantly attenuated IFN-β production as compared with control cells (Fig. 2 A). Similarly, the amount of IFN-β produced after LPS stimulation of HO-1–deficient macrophages was severely impaired (Fig. 2 A). We also examined whether HO-1 is required for the induction

of chemokine genes encoding RANTES, IP-10, MCP-1, MIP-1a, and MIP-1b in macrophages. HO-1–deficient and control TEPMs were stimulated with LPS for several time points and mRNA expression of all five chemokine genes was analyzed. Induction of genes encoding RANTES, IP-10, and MCP-1 was severely impaired in HO-1–deficient TEPMs compared with controls (Fig. 2 B). To eliminate the possibility that the observed defects are caused by an intrinsic defect in the expression of LPS/dsRNA receptors, we also analyzed induction of all known LPS/dsRNA receptors in response to LPS or polyI:C stimulation. Induction of genes encoding TLR4, TLR3, RIG-I, MDA5, and protein kinase regulated by RNA (PKR) occurred to the same extent in LPS- or polyI:C-treated macrophages from control and HO-$1^{M\text{-}KO}$ mice (Fig. S2). Finally, we questioned whether expression of IFN-β and HO-1 in macrophages trigger a "positive feedback loop" in which IFN-β (or TLR3 and/or TLR4 stimulation) up-regulates HO-1 and HO-1 mediates IFN-β expression. A similar phenomenon has been shown to mediate the antiinflammatory effect of IL-10 in macrophages in which IL-10 up-regulates HO-1 and HO-1 up-regulates IL-10 (17). To address this, we stimulated macrophages with LPS, polyI:C, and rIFN-β, and we analyzed HO-1 protein expression by Western blotting. We found that LPS treatment led to a significant induction of HO-1 protein expression, whereas polyI:C or rIFN-β did not induce HO-1 at all time points tested (Fig. S3).

HO-1 interacts with IRF3 and is required for its activation

A common feature of the IFN-β, RANTES, and IP-10 genes is that multiple transcriptional regulatory elements are required for their activation. For example, IFN-β gene expression requires the coordinate activation of the transcription factors IRF3 (26), NF-κB, and activating transcription factor 2/c-Jun (27). Various studies have established an essential role for IRF3 in LPS- and polyI:C-induced IFN-β, RANTES, and IP-10 gene expression (25, 28). We therefore sought to examine whether HO-1 deficiency interferes with the activation of these transcription factors. To determine NF-κB activity in the absence of HO-1 in polyI:C-induced gene expression, we stimulated TEPMs from control and HO-$1^{M\text{-}KO}$ mice with polyI:C for several time points, and nuclear extracts were analyzed for DNA binding activity by EMSA using a probe specific for the κB site. No significant difference was observed in the kinetics of NF-κB binding in HO-1–deficient extracts as compared with controls (Fig. 2 C), a finding that is in agreement with the results described in Fig. S1 B. We next assayed IRF3 DNA binding by EMSA using the IFN- and virus-inducible ISREs of the *Isg15* gene. Stimulation of control macrophages with polyI:C led to the detection of two complexes. The faster migrating complex corresponded to IRF3, whereas the slower complexes corresponded to IRF3 associated with the p300/CBP coactivators (29). In the absence of HO-1, IRF3 binding was reduced (Fig. 2 D). IRF3 primarily exists in two forms, a monomeric form that shuttles between

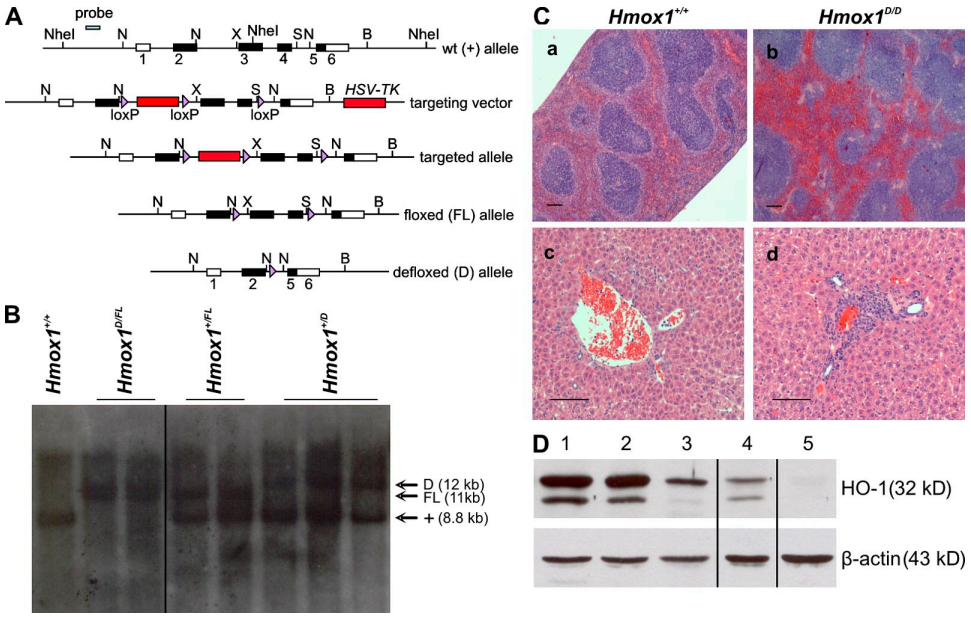

Figure 1. Generation and characterization of *Hmox1* conditional knockout mice. (A) The genomic structures of the mouse *Hmox1* gene, the targeting vector, and the floxed (FL) and defloxed (D) alleles are shown. Black boxes denote coding sequences. *Hmox1*$^{FL/FL}$ mice were crossed with the appropriate *Cre*-bearing deleter to obtain mice with ubiquitous or cell-type specific *Hmox1* deficiencies. (B) Southern blot analysis of offsprings. Genomic DNA was extracted digested with *Nhe*I (Nh), electrophoresed, and hybridized with the probe indicated in A. The blotting gave a single 8.8-kb band for the wild-type allele, a single 11-kb band for the floxed allele, and a single 12-kb band for the defloxed (D) allele. (C) Spleen (a and b) and hepatic (c and d) sections from 16-wk-old *Hmox*$^{+/+}$ and *Hmox*$^{D/D}$ mice stained with H&E. Bars, 100 µM. (D) Immunoblot analysis for the expression of HO-1 protein. TEPMs from *Hmox*$^{+/+}$ (1), *Hmox1*$^{FL/FL}$ (2), *LysM*$^{Cre/+}$*Hmox1*$^{FL/FL}$ (3), *LysM*$^{Cre/+}$*Hmox1*$^{D/FL}$ (4), and *Hmox*$^{D/D}$ (5) mice were stimulated with 50 µM hemin for 24 h, lysed, and blotted with anti–HO-1 antibody. The WCEs were simultaneously blotted with anti–β-actin antibody. Black lines indicate that intervening lanes have been spliced out.

the cytoplasm and the nucleus with a dominance of export versus import, and a dimeric form that results from its phosphorylation at the C terminus and is sequestered in the nucleus (29). To investigate whether HO-1 is involved in the phosphorylation of IRF3, we treated TEPMs from control and HO-1$^{M\text{-}KO}$ mice with polyI:C, and phosphorylation of IRF3 was detected by Western blotting using an antibody that specifically detects the phosphorylated form of IRF3. We found that activation of IRF3 was reduced in HO-1–deficient macrophages compared with controls (Fig. 2 E). In addition, IRF3 nuclear accumulation was detected by immunofluorescence. Consistent with the Western blotting and DNA-binding experiments, IRF3 nuclear accumulation was significantly reduced in macrophages lacking HO-1 (Fig. S4). To investigate whether HO-1 interacts with IRF3, we performed coimmunoprecipitation experiments using whole-cell extracts (WCEs) from control and HO-1$^{M\text{-}KO}$ macrophages treated with hemin to induce endogenous HO-1 protein and/or polyI:C. HO-1 immunoblot analysis on cell lysates that were immunoprecipitated with an anti-IRF3 antibody revealed that HO-1 interacts with IRF3 (Fig. 2 F). To determine whether HO-1 is also required for IRF7 activation, a transcription factor that also regulates IFN-β production, we stimulated control and HO-1–deficient macrophages with polyI:C and analyzed IRF7 mRNA induction. We found that IRF7 induction was similar in control and HO-1–deficient macrophages

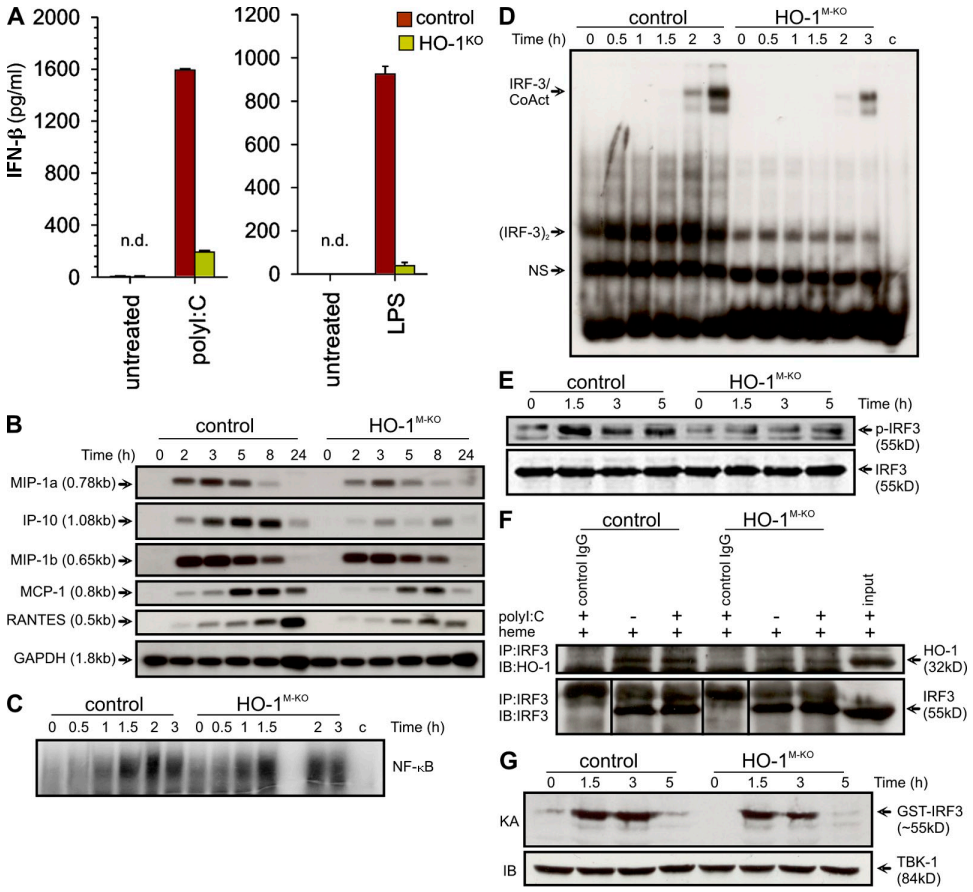

Figure 2. Defective IRF3 signaling and IFN-β production in HO-1–deficient macrophages. (A) ELISA of IFN-β production from BMDMs prepared from control (n = 3) and HO-1^{KO} (n = 3) mice; cells were left untreated or stimulated for 24 h with polyI:C or LPS. Data are means ± SD of three independent experiments. (B) Chemokine mRNA was analyzed by Northern blotting in LPS-treated TEPMs from control (n = 3) or HO-1$^{M\text{-}KO}$ (n = 3) mice. (C) Nuclear extracts (5 µg) from polyI:C-treated control or HO-1$^{M\text{-}KO}$ TEPMs were submitted to EMSA using an NF-κB–specific probe. (D) The same nuclear extracts were submitted to EMSA using the ISG15 ISRE. IRF3 associated with coactivators and IRF3 dimers are shown. To confirm binding specificity, 200-fold (lane 13) excess of unlabeled (cold) ISREs or NF-κB probes were present during the binding reaction. In C and D, c represents a 200-fold excess of the unlabeled (cold) ISRE probe present during the binding reaction to confirm binding specificity. (E) Control and HO-1–deficient TEPMs were stimulated with polyI:C for the indicated time points, and WCEs were blotted with antibodies to p-IRF3 and IRF3 as loading control. (F) Control and HO-1–deficient TEPMs were stimulated with heme and/or polyI:C, and cell lysates were immunoprecipitated with anti-IRF3 antibody or isotype control. The precipitates were resolved on SDS-PAGE and transferred onto a membrane. The blot was probed with anti–HO-1 antibody. (G) Kinase activity of TBK-1 was measured on WCEs from control and HO-1–deficient TEPMs by immune complex kinase assay (KA) using GST-IRF3 as substrate. For immunoblotting (IB), the top part of the gel was probed with a TBK-1 antibody to confirm equal amounts of the immunoprecipitated kinase. All experiments were performed at least two times. Black lines indicate that intervening lanes have been spliced out.

in response to polyI:C stimulation (Fig. S2). In addition, to determine whether lack of HO-1 affects the kinase activity of TBK-1, we performed a TBK-1 assay using cytoplasmic extracts from control and HO-1–deficient macrophages treated with polyI:C. We found that TBK-1 activity was similar in extracts derived from control and HO-1–deficient macrophages (Fig. 2 G). Collectively, these results show that HO-1 specifically interacts with IRF3 and affects its phosphorylation and subsequent nuclear translocation without affecting TBK-1 activity.

HO-1 is required for in vivo innate immune responses to TLR3

Recent studies have shown that *L. monocytogenes* can induce IFN-β once inside the cytoplasm of infected macrophages through the TBK-1–IRF3 signaling pathway (30, 31). IRF3-mediated induction of type I IFNs results in enhanced severity of *L. monocytogenes* infection (30). Furthermore, it has been shown that intravenous injection of polyI:C results in strong induction of type I IFNs that enhance pathogenicity

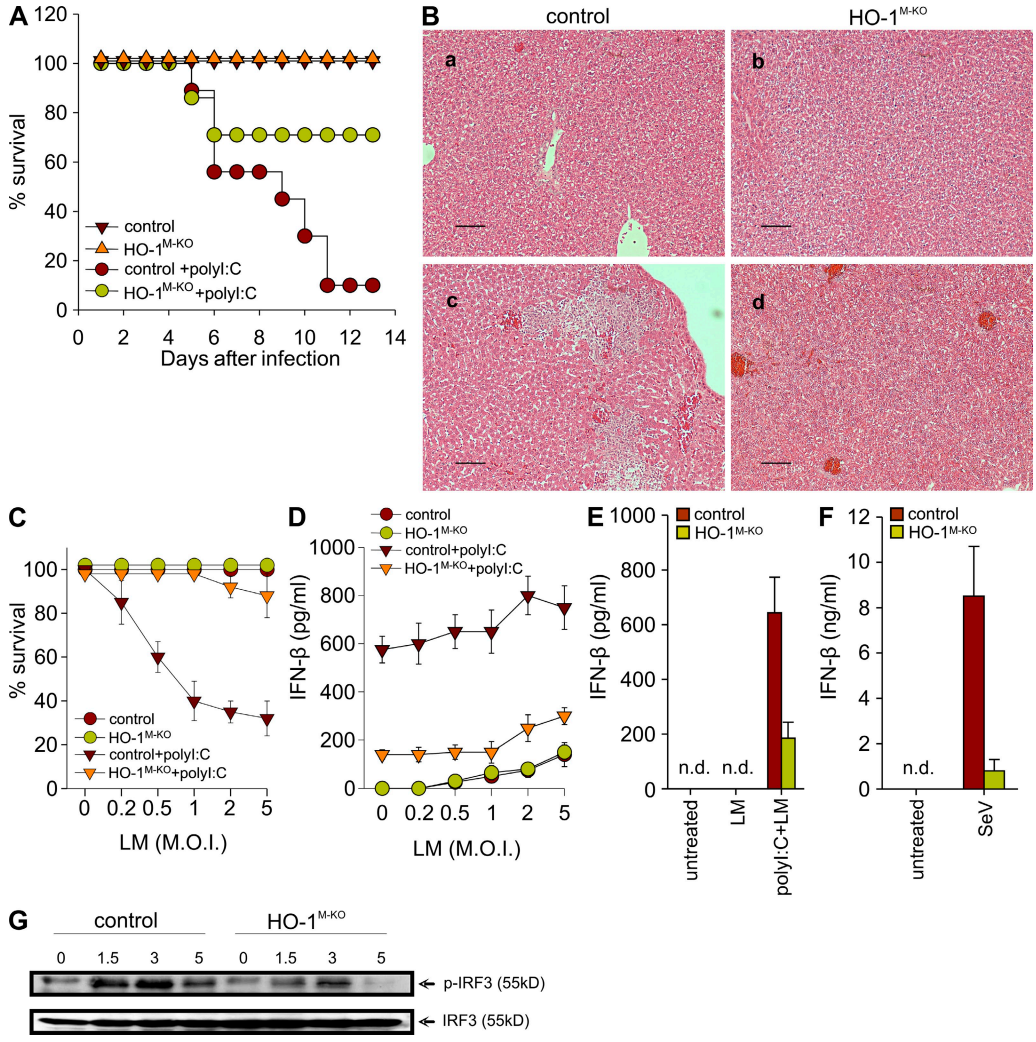

Figure 3. HO-1 in macrophages is required for the generation of immune responses to bacterial and viral infections. (A) Control and HO-1$^{M\text{-}KO}$ mice were infected intravenously with 10^5 CFU *L. monocytogenes* or with a combination of 10^5 CFU *L. monocytogenes* and 200 µg polyI:C, and viability was assayed daily for 14 d. Data are representative of two independent experiments (means ± SEM of nine mice per group). (B) Liver sections from control and HO-1$^{M\text{-}KO}$ mice infected intravenously with 10^5 CFU *L. monocytogenes* either in the absence (a and b) or presence (c and d) of 100 µg polyI:C were stained with H&E to assess inflammation. Representative sections from two independent experiments with five mice per group are shown. Bars, 100 µM. (C) TEPMs from control ($n = 3$) and HO-1$^{M\text{-}KO}$ ($n = 3$) mice were infected with *L. monocytogenes* at different MOIs (circles) or *L. monocytogenes* and polyI:C (triangles) as indicated, and cell survival was measured by crystal violet staining after 24 h. Data are representative of two independent experiments (means ± SEM of three mice per group). (D) IFN-β production was measured in supernatants from cultures in C (means ± SEM of three mice per group). (E) Control and HO-1$^{M\text{-}KO}$ mice were infected with 10^5 CFU *L. monocytogenes* or with a combination of 10^5 CFU *L. monocytogenes* and 200 µg polyI:C, and IFN-β was measured in sera collected 24 h later. Data are representative of two independent experiments (means ± SEM of six mice per group). (F) TEPMs from control ($n = 3$) and HO-1$^{M\text{-}KO}$ ($n = 3$) mice were infected with SeV, and IFN-β production was measured in supernatants after 24 h. Data are means ± SD of two independent experiments. (G) TEPMs from control ($n = 3$) and HO-1$^{M\text{-}KO}$ ($n = 3$) mice were infected with SeV for the indicated time points, and WCEs were probed for p-IRF3 and IRF3 as a loading control. Representative data from two independent experiments are shown. n.d., none detected.

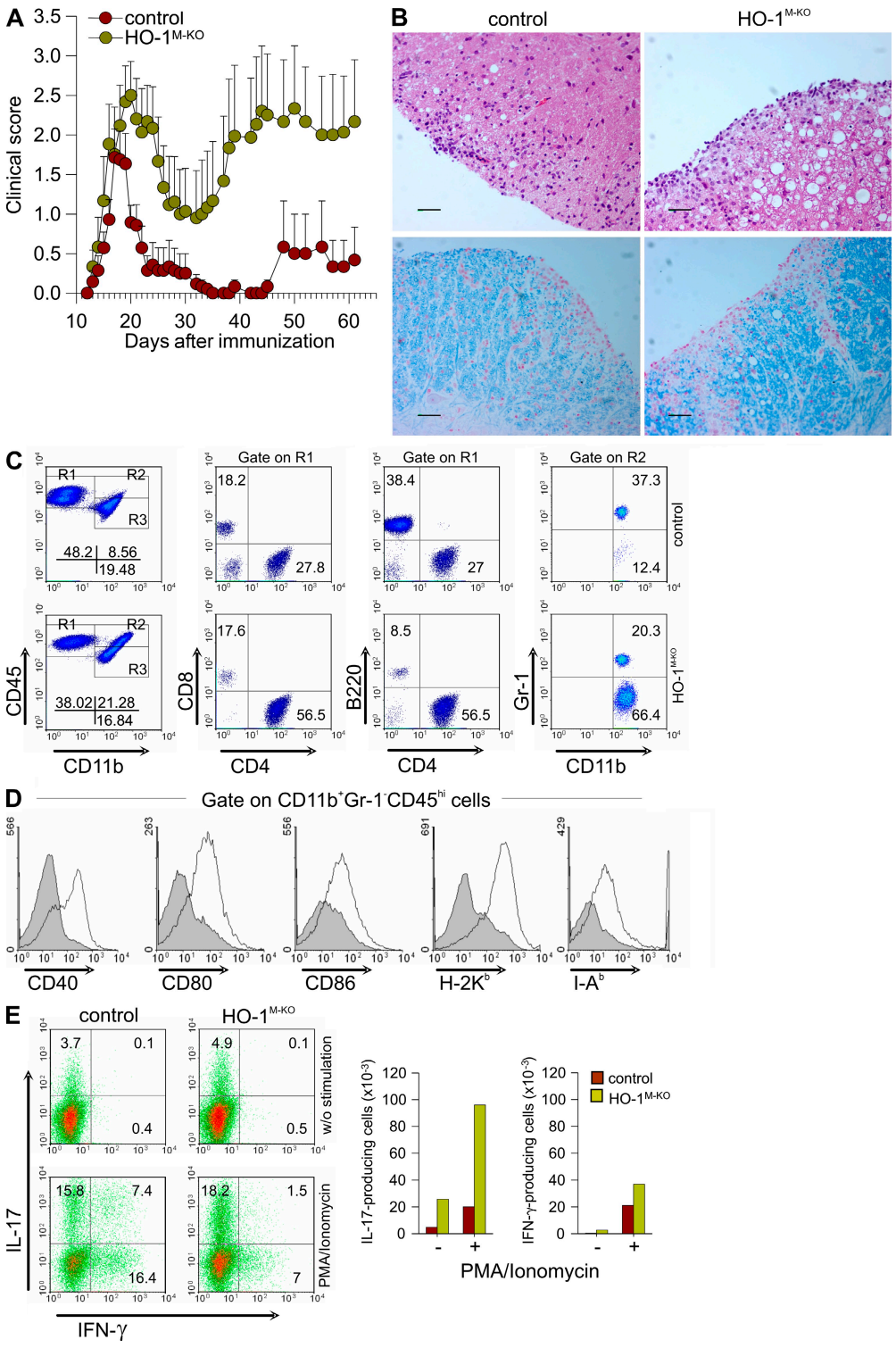

Figure 4. Macrophage-restricted ablation of HO-1 augments EAE. (A) Mean score of HO-1$^{M\text{-}KO}$ (n = 9) and littermate control (n = 9) mice at each measured time point. Results are representative of three different experiments (means ± SEM of nine mice per group). (B) Spinal cord sections from control (left) and HO-1$^{M\text{-}KO}$ (right) mice were stained with H&E to assess inflammation (top) and with LFB (bottom) to assess demyelination. Representative sections from two independent experiments with four mice per group are shown. Bars, 100 µM. (C) Immune cell infiltration into the CNS of control (n = 3) and HO-1$^{M\text{-}KO}$ (n = 3) mice. Infiltrates were stained with antibodies to CD45, CD11b, CD4, CD8, B220, and Gr-1 (R1 and R2 indicate gated areas). Numbers in quadrants indicate the percentages of cells in each. Data are representative of three independent experiments. (D) Co-stimulatory and MHC molecule expression in the CNS of HO-1$^{M\text{-}KO}$ mice. Immune cell infiltrates of control (shaded histograms; n = 4) and HO-1$^{M\text{-}KO}$ (open histograms;

during *L. monocytogenes* infection (30, 32). We have shown (Fig. 2) that HO-1–deficient macrophages have defective IRF3 signaling and IFN-β production, and we sought to determine whether HO-1 deficiency can protect mice from IFN-β–mediated sensitization to death during *L. monocytogenes* infection. We initially challenged control and HO-$1^{M\text{-}KO}$ mice with a sublethal dose of *L. monocytogenes*, and all mice remained healthy and viable (Fig. 3 A). Likewise, administration of polyI:C alone did not appear to influence the health status of the mice by day 14 (unpublished data). However, when mice were given a combination of a sublethal dose of *L. monocytogenes* along with polyI:C, only 10% of control mice remained viable, whereas 70% of HO-$1^{M\text{-}KO}$ mice survived the infection (Fig. 3 A). When a lower dose of polyI:C was used, only 40% of control mice remained viable, whereas all HO-$1^{M\text{-}KO}$ mice survived the infection (unpublished data). Histological analysis of control livers from polyI:C- and *L. monocytogenes*–coadministered mice revealed multiple parenchymal abscesses as compared with livers from control mice that were infected with *L. monocytogenes* alone (Fig. 3 B, a and c). Consistent with the survival studies, livers from HO-$1^{M\text{-}KO}$ mice with or without coadministration of polyI:C were relatively clear of tissue abscesses (Fig. 3 B, b and d). Infection-borne IFN-β plays an important role in sensitizing macrophages to *L. monocytogenes*–mediated cell death (31), and mice deficient in *IRF3* or *IFNAR1* are more resistant to *L. monocytogenes* infection because their splenocytes do not succumb to type I IFN–mediated apoptosis (30). To determine whether increased survival of HO-$1^{M\text{-}KO}$ mice is caused by reduced macrophage apoptosis, we infected control and HO-1–deficient macrophages with *L. monocytogenes* at different multiplicities of infection (MOIs) in the presence of polyI:C and measured cell death 24 h later. We found that 80% of HO-1–deficient cells survived the infection compared with 30% of control macrophages (Fig. 3 C). We also measured IFN-β production in culture supernatants from control and HO-1–deficient macrophages infected with *L. monocytogenes* in the presence of polyI:C. HO-1–deficient macrophages showed significantly attenuated IFN-β production as compared with control cells (Fig. 3 D), and this correlated with susceptibility to cell death. Finally, we measured IFN-β production in serum samples from control and HO-$1^{M\text{-}KO}$ mice challenged with a combination of a sublethal dose of *L. monocytogenes* along with polyI:C. In agreement with these in vitro data, IFN-β production was severely impaired in HO-$1^{M\text{-}KO}$ mice as compared with controls (Fig. 3 E). Collectively, these data suggest a major contribution of HO-1 to TLR3/IFN-β–mediated cell death during *L. monocytogenes* infections.

HO-1 is required for IFN-β production in response to virus infection

To gain insights into the biological relevance of macrophage HO-1 in virus infection–mediated responses, we infected macrophages from control and HO-$1^{M\text{-}KO}$ mice with SeV. Detection of paramyxoviruses, including SeV, has been attributed mainly to the RNA helicase RIG-I and, to a lesser extent, the RIG-I–like receptor MDA5 (8). We found that production of IFN-β was severely impaired in HO-1–deficient macrophages infected with SeV as compared with control cells (Fig. 3 F). In addition, HO-1–deficient macrophages displayed severely impaired phosphorylation of IRF3 in response to SeV infection as compared with control macrophages (Fig. 3 G). Collectively, these results indicate that HO-1 is indispensable for triggering antiviral responses against SeV infection.

Myeloid-specific ablation of HO-1 exacerbates EAE and is not suppressed by polyI:C-mediated IFN-β production

Multiple sclerosis is one of the diseases treated with IFN-β (33, 34), and recent studies show that IFN-β knockout mice have exacerbated EAE (35). More recent reports have also suggested a role for HO-1 in EAE, although the HO-1–mediated protective effects and their cellular basis remain largely unknown (20). When immunized with the encephalitogenic myelin oligodendrocyte glycoprotein ($MOG_{35\text{-}55}$) peptide, HO-$1^{M\text{-}KO}$ mice developed significantly more severe and chronic EAE with higher incidence compared with their control littermates (Fig. 4 A). Myeloid HO-1 deficiency did not affect the timing of disease onset but predominantly affected the severity and chronicity of EAE. Moreover, no differences in EAE severity between immunized $LysM^{Cre/+}$ mice and WT littermates were observed (Fig. S5), suggesting that expression of the Cre transgene in the *LysM* locus does not affect the course of EAE. To examine whether differences in EAE susceptibility and severity between HO-$1^{M\text{-}KO}$ and control mice lies in the priming of encephalitogenic T cells, we examined antigen-specific T cell responses in popliteal lymph nodes 8–10 d after infection. No differences were observed between HO-$1^{M\text{-}KO}$ and control mice regarding the capacity of T cells to proliferate (Fig. S6 A) or to produce IFN-γ and IL-4 (not depicted) in response to recall antigen. We next asked whether disease progression in HO-$1^{M\text{-}KO}$ mice may be caused by sustained autoreactivity of antigen-specific T cells. To address this, we examined the activation and differentiation of myelin-specific T cells in immunized HO-$1^{M\text{-}KO}$ mice during the late relapse and remission stages. Splenocytes from HO-$1^{M\text{-}KO}$ mice showed a fourfold higher proliferation compared with control cells and produced much higher levels of

$n = 4$) mice were stained with antibodies to CD40, CD80, CD86, H-$2K^b$, and I-A^b. (E) Spinal cord cells from control ($n = 3$) and HO-$1^{M\text{-}KO}$ ($n = 3$) mice were harvested 25 d after infection, and the percentage of live $CD4^+$ T cells that express intracellular IFN-γ and IL-17 with or without stimulation (PMA/ionomycin) was measured by flow cytometry analysis. The numbers in each quadrant represent the frequency of $CD4^+$ T cells expressing IFN-γ and/or IL-17. Quantification and absolute numbers of IFN-γ and IL-17–producing T cells in the spinal cords of control and HO-$1^{M\text{-}KO}$ mice are also shown. Data are representative of three independent experiments.

IFN-γ and TNF (Fig. S6, B–D) in response to MOG. Histological analysis of spinal cords of HO-1$^{M\text{-}KO}$ and control mice 25 d after infection showed that HO-1$^{M\text{-}KO}$ mice had significantly more cellular infiltration and demyelination throughout the spinal cord compared with control mice (Fig. 4 B). Flow cytometry analysis of the immune cell infiltrates showed that HO-1$^{M\text{-}KO}$ mice had increased numbers of inflammatory cells, including CD4$^+$ and CD8$^+$ T cells, macrophages, and granulocytes, than did control mice (Fig. 4 C and Table S1). Infiltrating macrophages (CD45^{high} CD11b$^+$Gr1$^-$) showed increased expression of CD40, CD80, CD86, H-2K^b, and I-A^b (Fig. 4 D) as compared with controls. In the CNS of HO-1$^{M\text{-}KO}$ mice, we observed a fivefold increase in the numbers of IL-17–producing CD4$^+$ T cells and a twofold increase in the numbers of IFN-γ–producing CD4$^+$ T cells (Fig. 4 E) with an IL-17/IFN-γ ratio of >2:1. Recent studies show that a preferential activation of the MyD88-independent, type I IFN–inducing TLR pathway has immunomodulatory potential in EAE and that disease suppression is associated with increased levels of IFN-β (36). Touil et al. performed in vivo neutralization experiments and showed that EAE protection by polyI:C was reversed by an anti–IFN-β antibody, indicating a role for IFN-β in mediating this effect of polyI:C. To test whether exacerbation of EAE in HO-1$^{M\text{-}KO}$ mice was associated with defective IFN-β production from macrophages, immunized HO-1$^{M\text{-}KO}$ and control mice were administered polyI:C (30 μg/mouse/day) or PBS during the induction phase of EAE (days 5 and 8 after infection). Clinical signs of disease were suppressed in control mice that received polyI:C as compared with PBS-treated control mice. On the contrary, polyI:C-treated HO-1$^{M\text{-}KO}$ mice developed severe and chronic EAE that was similar to PBS-treated HO-1$^{M\text{-}KO}$

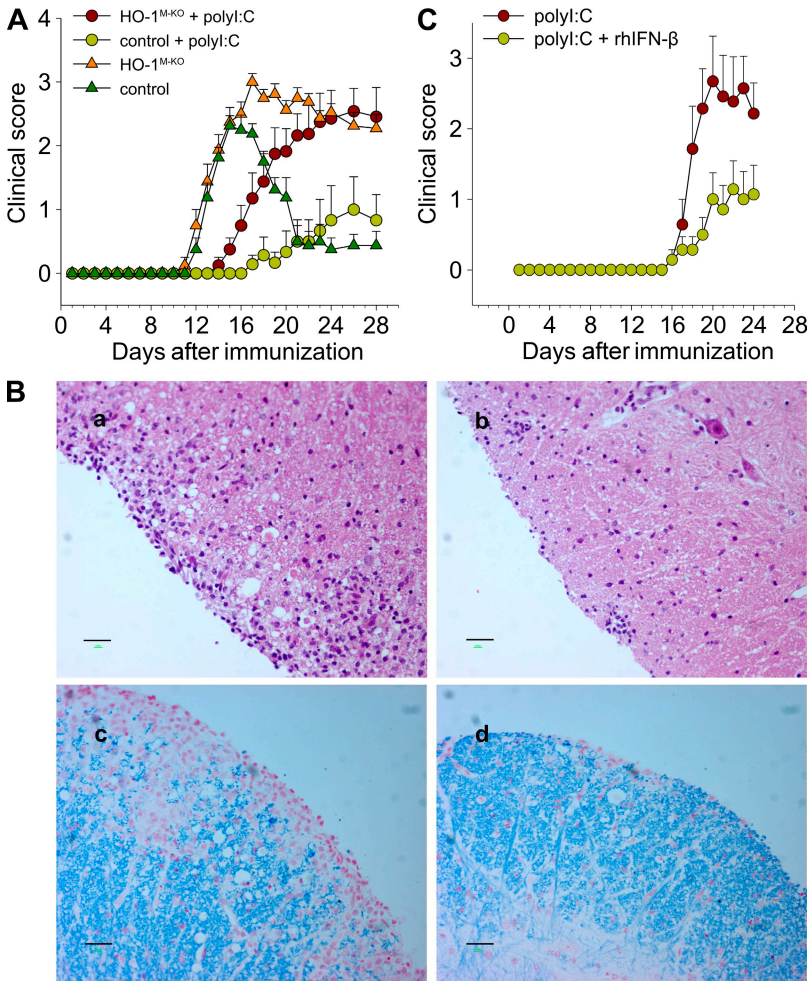

Figure 5. Clinical and histological effects of polyI:C administration in HO-1$^{M\text{-}KO}$ mice with EAE. (A) Control (n = 9) and HO-1$^{M\text{-}KO}$ (n = 10) mice were treated with intraperitoneal injections of polyI:C or PBS on days 5 and 8 after infection. Data are representative of three independent experiments (means ± SEM of at least nine mice per group). (B) Spinal cord sections from immunized, polyI:C-treated HO-1$^{M\text{-}KO}$ (a and c) and control (b and d) mice 28 d after infection were stained with H&E and LFB. Representative sections from two independent experiments with five mice per group are shown. Bars, 100 μM. (C) Immunized HO-1$^{M\text{-}KO}$ mice were treated with intraperitoneal injections of polyI:C on days 5 and 8 after infection, and were either treated with PBS or with rhIFN-β starting from day 9 after infection and continuing over a period of 14 d. Data are representative of two independent experiments (means ± SEM of 10 mice per group).

mice (Fig. 5, A and B). We then asked whether treatment with rIFN-β can inhibit the clinical symptoms of EAE in myeloid HO-1–deficient mice. For this, immunized HO-$1^{M\text{-}KO}$ mice were administered polyI:C and were treated with PBS or rIFN-β (200,000 IU/day) starting from day 9 after infection and continuing over a period of 14 d. Clinical signs of disease were significantly suppressed in HO-$1^{M\text{-}KO}$ mice that received polyI:C and rIFN-β as compared with HO-$1^{M\text{-}KO}$ mice that received polyI:C alone (Fig. 5 C). Collectively, these data show that absence of myeloid HO-1 exacerbates EAE characterized by enhanced infiltration of macrophages and Th17 cells, and a nonregressing myelin-specific T cell reactivity. Furthermore, we showed that regulation of autoimmune disease in HO-$1^{M\text{-}KO}$ mice critically depends on IFN-β production, demonstrating an essential requirement for HO-1 in this pathway.

DISCUSSION

HO-1 is known to be involved in a vast array of pathophysiological conditions (37, 38). HO-1 expression or CO administration mediate potent antiinflammatory effects in monocytes and/or macrophages, probably restraining these cells from inducing tissue injury and modulating their role in the initiation of immune responses. Several studies have shown the protective effects of the HO-1/CO system; CO suppresses the proinflammatory and promotes the antiinflammatory response of macrophages, a cell type that controls the balance of inflammation in many conditions. Macrophages stimulated with bacterial LPS produce several proinflammatory cytokines, including TNF (39), as well as antiinflammatory cytokines such as IL-10 (40). If macrophages overexpress HO-1 or are exposed to CO in vitro before stimulation with LPS, the proinflammatory response is markedly inhibited, whereas the antiinflammatory response is enhanced (16, 41). In addition, Lee and Chau identified a potential interplay between IL-10 and HO-1 in the inhibition of LPS-induced inflammatory responses and provided evidence that HO-1 mediates the antiinflammatory function of IL-10 both in vivo and in vitro, and that IL-10 and HO-1 activate a positive feedback circuit to amplify the antiinflammatory response (17).

In this work, we have provided genetic evidence that identifies a novel function for myeloid HO-1 as an upstream mediator of the IRF3/IFN-β response, orchestrating many subsequent processes central to innate as well as adaptive immune responses. Our data indicate that HO-1 forms a complex with IRF3 and is essential for IRF3 activation and subsequent gene expression in response to TLR3/TLR4 stimulation. Although HO-1 can bind to its isoenzyme HO-2 (42), no reports demonstrate binding of HO-1 to known transcriptions factors. A recent study by Lin et al. has shown that HO-1 is detected in the nucleus of cultured cells after exposure to hypoxia, and that HO-1 protein altered binding of transcription factors involved in oxidative stress (43). HO-1 is not a traditional transcription factor with DNA binding motifs (44); therefore, direct transcriptional activation is less likely to occur. However, HO-1 could bind to other proteins,

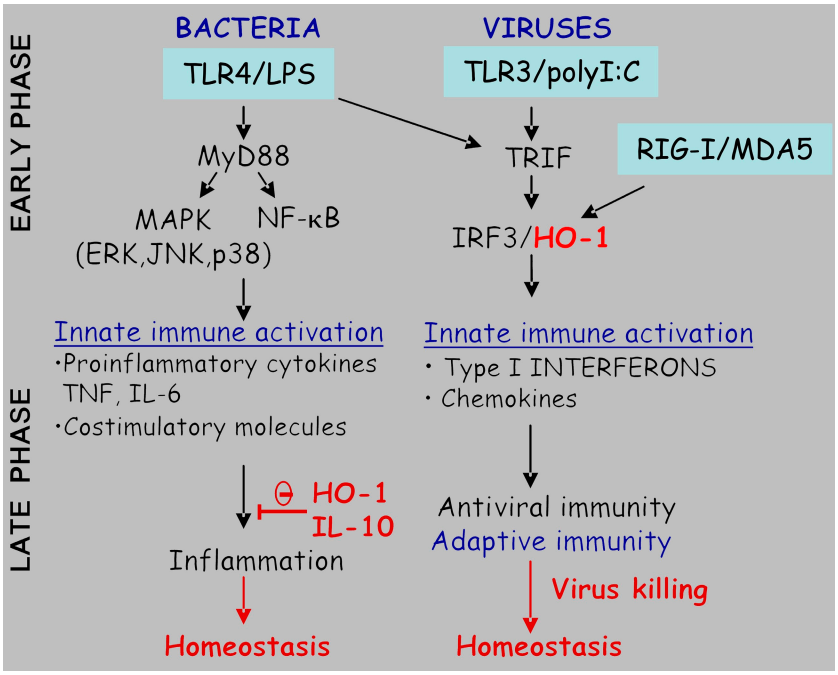

Figure 6. A proposed model implicating myeloid HO-1–mediated regulation of immune cytokines and responses. Upon TLR4 stimulation, HO-1 is not required for the early phase MyD88- or TRIF-dependent activation of MAPKs and NF-κB but is required for the suppression of inflammatory responses at later time points. On the other hand, early phase activation of the TRIF–IRF3 and RIG-I–IRF3 pathways requires HO-1 for the production of antiviral cytokines, TLR3/4 primary response genes, and the development of adaptive immune responses.

serving as the non-DNA binding protein of a transcriptional factor complex, or could be a scaffold protein, acting as a chaperone for unstable client proteins and keeping them poised for activation. It remains to be determined how HO-1 modulates transcription factor activity and if modulation of these factors is mediated by HO-1 protein or its byproducts, such as CO. Recent reports have also suggested a role for CO in the regulation of TLR signaling pathways. CO treatment was shown to negatively control TLR signaling by inhibiting translocation of TLRs to lipid rafts (10). In the same study, although CO inhibited TLR4 signaling and subsequent IFN-β production after LPS stimulation, it did not affect TLR3-dependent signaling in macrophages in response to polyI:C treatment. Therefore, it appears that the observed effects of CO on the TLR3 signaling pathway are independent of the HO-1 protein function. This is supported by the observation of Hegazi et al. (11) that CO inhibits the synergistic activation of IL-12 p40 and inducible nitric oxide synthase by LPS/IFN-γ through selective inhibition of IRF8. The immunological effects of CO required HO-1, and in the absence of functional HO-1, the inhibitory action of CO on IRF8 and IL-12 p40 expression was lost. In agreement with this, we have not observed a defect in IRF8 activation in macrophages from HO-$1^{M\text{-}KO}$ mice in response to LPS/IFN-γ (unpublished data). These results suggest that the products of the HO-1 pathway impart antiinflammatory effects via different modes of action and that HO-1 may have a cytoprotective role independent of its two major metabolic byproducts. Collectively, these findings reveal a multifaceted role for HO-1 in immune responses, presented schematically in Fig. 6; in response to bacterial or viral stimuli, HO-1 is required for early activation of the type I IFN–inducing pathway and subsequent development of antiviral or adaptive immunity. At a later time point, HO-1, through CO production, acts to inhibit the proinflammatory response and enhance the antiinflammatory effects of IL-10.

The physiological significance of the HO-1–mediated type I IFN induction was shown using a bacterial/viral infection model in which polyI:C dramatically sensitizes mice to *L. monocytogenes* inoculation in an IFNAR1-dependent manner (30). Even though the complete mechanism by which type I IFNs inhibit host immunity to *L. monocytogenes* is likely complex because of the pleiotropic cellular effects mediated by these cytokines, there is evidence showing that IRF3-dependent production of IFN-β by the infected macrophages induces apoptosis in neighboring cells and, possibly, macrophages themselves (30, 31). In accordance, mice with myeloid-specific HO-1 deficiency were resistant to polyI:C/*L. monocytogenes* infection, and this was associated with reduced IFN-β production in vivo. In addition, we showed that HO-1 deficiency exacerbated an autoimmune condition that is dependant on endogenous IFN-β production. Absence of myeloid HO-1 exacerbated EAE in mice, and this was associated with enhanced leukocyte accumulation within the CNS, including Th17 cells and nonregressing myelin-specific T cell responses. It was recently shown that activation of the TLR3–type I IFN–inducing pathway by polyI:C suppresses EAE through induction of endogenous IFN-β. IFN-β is used for the treatment of multiple sclerosis; its mechanisms of action include induction of IL-10, inhibition of the expansion of encephalitogenic T cells (45), reduced production of inflammatory cytokines, and reduction of blood–brain barrier permeability (46, 47). In the absence of myeloid HO-1, activation of the type I IFN–inducing pathway by polyI:C treatment did not suppress the development of disease in immunized HO-$1^{M\text{-}KO}$ mice. In contrast, rIFN-β–treated HO-$1^{M\text{-}KO}$ mice displayed low clinical scores, suggesting that the protective effects of HO-1 are mediated through endogenous IFN-β induction.

In conclusion, our findings demonstrate a multilayered functioning of HO-1 in immunity and disease, with an early critical involvement of this molecule in IRF3-driven innate immune activation and with subsequent enzymatic activities that are known to confer cell and tissue protective antiinflammatory, antiapoptotic, antiproliferative, and antioxidant effects (37). Differential modulation of such enzymatic and/or signaling activities of HO-1 may hold clues for more effective therapeutic uses of this molecule in a range of immune pathologies.

MATERIALS AND METHODS

Generation of *Hmox1* conditional knockout mice. Phage clones containing mouse *Hmox1* were isolated by screening of a 129/Svev genomic library (UK Human Genome Mapping Project Resource Centre) with a probe corresponding to the 5′ end of mouse HO-1 cDNA. A targeting vector was designed to flank exons 3 and 4, with two *lox*P sites. The floxed neomycin-resistance gene fragment was inserted into intron 2 of *Hmox1*. A 5.2-kb *Not*I-*Not*I fragment (exons 1 and 2) was used as the 5′ homology region; a 2.1-kb *Xho*I-*Spe*I fragment, which contains exons 3 and 4 of *Hmox1*, was inserted between the two *lox*P sites; and a 2.1-kb *Nhe*I-*Bam*HI fragment was used as the 3′ homology region. The herpes simplex virus thymidine kinase gene was used for negative selection of clones with random integration. A total of 20 μg of linearized vector was electroporated into 129/3 embryonic stem cells (provided by N. Brockdorff, University of Oxford, Oxford, England, UK). After positive and negative selection with G418 and gancyclovir, drug-resistant clones were picked up and screened by PCR and Southern blot analysis. These clones were individually microinjected into blastocysts derived from C57BL/6 mice and were transferred to pseudopregnant females. Matings of chimeric male mice to C57BL/6 female mice resulted in transmission of the floxed allele to the germline. Chimeric mice were bred to CMV-Cre transgenic mice (21) to remove the neomycin cassette. All mice were housed under specific pathogen-free conditions, and animal protocols used in this study were approved by the Institutional Animal Care and Use Committee of the Biomedical Sciences Research Center "Alexander Fleming."

Cell cultures and reagents. TEPMs and BMDMs were grown as previously described (1, 48). For the IFN-β (PBL Biomedical Laboratories), IL-6 (Thermo Fisher Scientific), and TNF (provided by W. Buurman, Nutrition and Toxicology Research Institute Maastricht, Maastricht, Netherlands) ELISA assays, macrophage cultures (5×10^5 cells/well) were incubated with 1 μg/ml LPS (*Salmonella enteriditis*; Sigma-Aldrich) or 100 μg/ml polyI:C (GE Healthcare).

Viral infections. SeV Cantell strain was provided by D. Thanos (Academy of Athens, Athens, Greece) and was used to infect macrophages (10^6 cells/ml) at 100 hemagglutination U/ml for the time points indicated in the figures.

Bacterial infections and assays to measure cell death. Preparation of *L. monocytogenes* and in vivo infections were previously described (30). Macrophages (10^6 cells/well) were infected with *L. monocytogenes* (derived from

overnight culture) at different MOIs and incubated for 1 h at 37°C. Extracellular bacteria were subsequently killed with 50 μg/ml of gentamycin-containing medium. After another 60 min, the medium was changed to medium containing 10 μg/ml gentamycin, and the assay was incubated for 24 h. For crystal violet staining, cells were incubated for 20 min in 0.2% crystal violet in 20% methanol, as previously described (31).

Immunoblot analysis, immunoprecipitation, and immunofluorescence staining. Immunoprecipitation and immunoblot analysis were performed as previously described (16). Membranes were blotted with antibodies to HO-1 (Assay Designs), p-Jnk, total Jnk, total p38, p-Erk, actin (Santa Cruz Biotechnology, Inc.), p-IκBα, p-p38, total IκBα, p-IRF3, p-IKKα/β, IKKα and IKKβ (Cell Signaling Technology), total IRF3 (Invitrogen), and TBK-1 (Millipore). For immunofluorescence staining, macrophages were stimulated with LPS or polyI:C for the periods indicated in the figures, permeabilized, and incubated with rabbit anti-IRF3 (Invitrogen).

In vitro kinase assay. The TBK-1 in vitro kinase assay was performed as previously described (49). Materials (polyclonal anti–TBK-1 antibody and glutathione S-transferase (GST)–IRF3 plasmid) were provided by J. Hiscott (McGill University, Montreal, Canada). GST-IRF3 was expressed in *E. coli* strain BL21(DE3)pLysS, and GST-IRF3 protein was purified using the MagneGST Protein Purification System (Promega) according to the manufacturer's instructions.

EMSA. 5×10^6 TEPMs were treated with stimuli for various periods. Nuclear extracts were purified and EMSA was performed as previously described (29). The sequences of the oligonucleotides used for the ISG15 gene are as follows, with the ISRE sequence underlined: ISG15F (5′-GATCCTCGGGAAAGGGAAACCGAAACTGAAGCC-3′) and ISG15R (5′-CGGGGCTTCAGTTTCGGTTTCCCTTTCCCGAG-3′). The sequences of the oligonucleotides used for NF-κB with two tandemly positioned NF-κB binding sites (underlined) were as follows: NFκBF (5′-ATCAGGGACTTTCCGCTGGGGACTTT-3′) and NFκBR (5′-CGGAAAGTCCCCAGCGGAAAGTCCCT-3′).

Northern blot and RT-PCR analysis. RNA was isolated using TRIzol reagent (Invitrogen). For Northern blot analysis, 20 μg of total RNA was separated in a 1.2% agarose-formaldehyde gel, transferred to nitrocellulose, and hybridized to ^{32}P-labeled DNA probes. MCP1, MIP-1a, MIP-1b, RANTES, IP-10, and GAPDH probes were amplified from reverse-transcribed cDNA using the following oligonucleotides: MCP1f (5′-AGCACCAGCACCAGCCAACT-3′), MCP1r (5′-TTCCTTCTTGGGGTCAGCAC-3′), MIP-1af (5′-TCTCCACCACTGCCCTTGCT-3′), MIP-1ar (5′-CTCAGGCATTCAGTTCCAGG-3′), MIP-1bf (5′-GCAAACCTAACCCCGAGCAA-3′), MIP-1br (5′-TCCTGAAGTGGCTCCTCCTG-3′), RANTESf (5′-GCCCTCACCATCATCCTCAC-3′), RANTESr (5′-ATCCCATTTTCCCAGGACC-3′), IP-10f (5′-GCCGTCATTTTCTGCCTCAT-3′), IP-10r (5′-TCGCACCTCCACATAGCTTA-3′), GAPDHf(5′-TTAGCACCCCTGGCCAAGG-3′), and GAPDHr (5′-CTTACTCCTTGGAGGCCATG-3′).

For quantitative real-time RT-PCR, 5 μg of total RNA was used to make cDNA templates using M-MLV RT (Promega) and oligo-dT primers after treatment with RQ1 DNase I (Promega). Real-time PCR was performed on Chromo4 Real-Time PCR detection system (Bio-Rad Laboratories) using Platinum SYBR Green (Invitrogen). All data were normalized to β2-microglobulin (β2m) expression. Amplification conditions were 95°C for 4 min, followed by 40 cycles of 94°C for 30 s, 55°C for 30 s, and 72°C for 30 s. TLR4, TLR3, RIG-I, MDA5, PKR, and β2m cDNAs were amplified using the following primers: TLR4f (5′-AAAAGTGAGAATGCTAAGGT-3′), TLR4r (5′-CGCAACGCAAGGATTTTATT-3′), TLR3f (5′-TGACGCACCTGTTCTCTATC-3′), TLR3r (5′-CGCAACGCAAGGATTTTATT-3′), RIG-If (5′-AGACAAAGAGGAGGAGAGCCG-3′), RIG-Ir (5′-ACGCCCAGTCAGTATGCCAG-3′), MDA5f (5′-AGGAGGCAGTCTATAACAAC-3′), MDA5r (5′-ATGGATTTTCTCTGGTGTCA-3′), PKRf (5′-TTGGCTTAGGTGGATTTGGT-3′), PKRr (5′-TTCTGTTTCTCATCCATTGC-3′), B2Mf (5′-TTCTGGTGCTTGTCTCACTGA-3′), and B2Mr (5′-CAGTATGTTCGGCTTCCCATTC-3′).

Induction of EAE and rIFN-β treatment. Induction of EAE was performed as previously described (48) with 50 μg of rat MOG peptide in CFA containing a total of 1 mg H37Ra per mouse. rhIFN-β (Betaferon; Schering-Plough) was administered for 14 d using mini-osmotic pumps (model 2002; Alzet).

Spinal cord flow cytometry. Spinal cord cells were isolated as previously described (50). For flow cytometry, cells were stained for 30 min at 4°C with various primary antibodies (BD). Cells were analyzed with a flow cytometer (FACSCalibur; BD).

Histological analysis. Mice were perfused with PBS and spinal cords were fixed in 10% buffered formalin. The spinal cords were dissected and paraffin embedded before staining with hematoxylin and eosin (H&E) to assess inflammation, and luxol fast blue (LFB) to assess demyelination.

Online supplemental material. Fig. S1 shows activation of the MAPK and NF-κB signaling cascades and proinflammatory cytokine production in HO-1–deficient macrophages. Fig. S2 depicts the induction of genes encoding LPS/dsRNA receptors in HO-1–deficient macrophages. Fig. S3 shows that HO-1 is not induced by IFN-β or dsRNA and is induced by LPS. Fig. S4 shows that nuclear translocation of IRF3 is impaired in HO-1–deficient macrophages. Fig. S5 depicts the development of EAE in $LysM^{Cre/+}$ knockin and WT mice. Fig. S6 depicts the proliferation and cytokine production of LNs and spleen cells from HO-$1^{M\text{-}KO}$ and control mice immunized with $MOG_{35\text{-}55}$. Table S1 shows the quantification of CNS-infiltrating cells during the chronic phase of EAE. Online supplemental material is available at http://www.jem.org/cgi/content/full/jem.20081582/DC1.

We thank Dr. D. Thanos for providing the SeV, Prof. J. Hiscott for reagents for the TBK-1 assay, Dr. Neil Brockdorff for providing 129/3 embryonic stem cells, and S. Lalos and P. Athanasakis for technical support.

This work was supported by European Commission grants QLK3-CT-2001-00422, MRTN-CT-2004-005693, LSHB-CT-2004-005276, and LSHG-CT-2005-005203 to G. Kollias.

The authors declare no conflicting financial interests.

Submitted: 18 July 2008
Accepted: 8 April 2009

REFERENCES

1. Alexopoulou, L., A.C. Holt, R. Medzhitov, and R.A. Flavell. 2001. Recognition of double-stranded RNA and activation of NF-kappaB by Toll-like receptor 3. *Nature*. 413:732–738.
2. Poltorak, A., X. He, I. Smirnova, M.Y. Liu, C. Van Huffel, X. Du, D. Birdwell, E. Alejos, M. Silva, C. Galanos, et al. 1998. Defective LPS signaling in C3H/HeJ and C57BL/10ScCr mice: mutations in Tlr4 gene. *Science*. 282:2085–2088.
3. Hemmi, H., T. Kaisho, O. Takeuchi, S. Sato, H. Sanjo, K. Hoshino, T. Horiuchi, H. Tomizawa, K. Takeda, and S. Akira. 2002. Small anti-viral compounds activate immune cells via the TLR7 MyD88-dependent signaling pathway. *Nat. Immunol.* 3:196–200.
4. Heil, F., H. Hemmi, H. Hochrein, F. Ampenberger, C. Kirschning, S. Akira, G. Lipford, H. Wagner, and S. Bauer. 2004. Species-specific recognition of single-stranded RNA via toll-like receptor 7 and 8. *Science*. 303:1526–1529.
5. Hemmi, H., O. Takeuchi, T. Kawai, T. Kaisho, S. Sato, H. Sanjo, M. Matsumoto, K. Hoshino, H. Wagner, K. Takeda, and S. Akira. 2000. A Toll-like receptor recognizes bacterial DNA. *Nature*. 408: 740–745.
6. Akira, S., and K. Takeda. 2004. Toll-like receptor signalling. *Nat. Rev. Immunol.* 4:499–511.

7. Takeda, K., and S. Akira. 2005. Toll-like receptors in innate immunity. *Int. Immunol.* 17:1–14.
8. Kato, H., O. Takeuchi, S. Sato, M. Yoneyama, M. Yamamoto, K. Matsui, S. Uematsu, A. Jung, T. Kawai, K.J. Ishii, et al. 2006. Differential roles of MDA5 and RIG-I helicases in the recognition of RNA viruses. *Nature.* 441:101–105.
9. Kumar, H., T. Kawai, H. Kato, S. Sato, K. Takahashi, C. Coban, M. Yamamoto, S. Uematsu, K.J. Ishii, O. Takeuchi, and S. Akira. 2006. Essential role of IPS-1 in innate immune responses against RNA viruses. *J. Exp. Med.* 203:1795–1803.
10. Nakahira, K., H.P. Kim, X.H. Geng, A. Nakao, X. Wang, N. Murase, P.F. Drain, M. Sasidhar, E.G. Nabel, T. Takahashi, et al. 2006. Carbon monoxide differentially inhibits TLR signaling pathways by regulating ROS-induced trafficking of TLRs to lipid rafts. *J. Exp. Med.* 203:2377–2389.
11. Hegazi, R.A., K.N. Rao, A. Mayle, A.R. Sepulveda, L.E. Otterbein, and S.E. Plevy. 2005. Carbon monoxide ameliorates chronic murine colitis through a heme oxygenase 1–dependent pathway. *J. Exp. Med.* 202:1703–1713.
12. Yachie, A., Y. Niida, T. Wada, N. Igarashi, H. Kaneda, T. Toma, K. Ohta, Y. Kasahara, and S. Koizumi. 1999. Oxidative stress causes enhanced endothelial cell injury in human heme oxygenase-1 deficiency. *J. Clin. Invest.* 103:129–135.
13. Poss, K.D., and S. Tonegawa. 1997. Heme oxygenase 1 is required for mammalian iron reutilization. *Proc. Natl. Acad. Sci. USA.* 94:10919–10924.
14. Poss, K.D., and S. Tonegawa. 1997. Reduced stress defense in heme oxygenase 1-deficient cells. *Proc. Natl. Acad. Sci. USA.* 94:10925–10930.
15. Morse, D., S.E. Pischke, Z. Zhou, R.J. Davis, R.A. Flavell, T. Loop, S.L. Otterbein, L.E. Otterbein, and A.M. Choi. 2003. Suppression of inflammatory cytokine production by carbon monoxide involves the JNK pathway and AP-1. *J. Biol. Chem.* 278:36993–36998.
16. Otterbein, L.E., F.H. Bach, J. Alam, M. Soares, H. Tao Lu, M. Wysk, R.J. Davis, R.A. Flavell, and A.M. Choi. 2000. Carbon monoxide has anti-inflammatory effects involving the mitogen-activated protein kinase pathway. *Nat. Med.* 6:422–428.
17. Lee, T.S., and L.Y. Chau. 2002. Heme oxygenase-1 mediates the anti-inflammatory effect of interleukin-10 in mice. *Nat. Med.* 8:240–246.
18. Pamplona, A., A. Ferreira, J. Balla, V. Jeney, G. Balla, S. Epiphanio, A. Chora, C.D. Rodrigues, I.P. Gregoire, M. Cunha-Rodrigues, et al. 2007. Heme oxygenase-1 and carbon monoxide suppress the pathogenesis of experimental cerebral malaria. *Nat. Med.* 13:703–710.
19. Zwerina, J., S. Tzima, S. Hayer, K. Redlich, O. Hoffmann, B. Hanslik-Schnabel, J.S. Smolen, G. Kollias, and G. Schett. 2005. Heme oxygenase 1 (HO-1) regulates osteoclastogenesis and bone resorption. *FASEB J.* 19:2011–2013.
20. Chora, A.A., P. Fontoura, A. Cunha, T.F. Pais, S. Cardoso, P.P. Ho, L.Y. Lee, R.A. Sobel, L. Steinman, and M.P. Soares. 2007. Heme oxygenase-1 and carbon monoxide suppress autoimmune neuroinflammation. *J. Clin. Invest.* 117:438–447.
21. Schwenk, F., U. Baron, and K. Rajewsky. 1995. A cre-transgenic mouse strain for the ubiquitous deletion of loxP-flanked gene segments including deletion in germ cells. *Nucleic Acids Res.* 23:5080–5081.
22. Clausen, B.E., C. Burkhardt, W. Reith, R. Renkawitz, and I. Forster. 1999. Conditional gene targeting in macrophages and granulocytes using LysMcre mice. *Transgenic Res.* 8:265–277.
23. Hiscott, J., N. Grandvaux, S. Sharma, B.R. Tenoever, M.J. Servant, and R. Lin. 2003. Convergence of the NF-kappaB and interferon signaling pathways in the regulation of antiviral defense and apoptosis. *Ann. NY Acad. Sci.* 1010:237–248.
24. Honda, K., and T. Taniguchi. 2006. IRFs: master regulators of signalling by Toll-like receptors and cytosolic pattern-recognition receptors. *Nat. Rev. Immunol.* 6:644–658.
25. Doyle, S., S. Vaidya, R. O'Connell, H. Dadgostar, P. Dempsey, T. Wu, G. Rao, R. Sun, M. Haberland, R. Modlin, and G. Cheng. 2002. IRF3 mediates a TLR3/TLR4-specific antiviral gene program. *Immunity.* 17:251–263.
26. Goodbourn, S., and T. Maniatis. 1988. Overlapping positive and negative regulatory domains of the human beta-interferon gene. *Proc. Natl. Acad. Sci. USA.* 85:1447–1451.
27. Du, W., D. Thanos, and T. Maniatis. 1993. Mechanisms of transcriptional synergism between distinct virus-inducible enhancer elements. *Cell.* 74:887–898.
28. Sakaguchi, S., H. Negishi, M. Asagiri, C. Nakajima, T. Mizutani, A. Takaoka, K. Honda, and T. Taniguchi. 2003. Essential role of IRF-3 in lipopolysaccharide-induced interferon-beta gene expression and endotoxin shock. *Biochem. Biophys. Res. Commun.* 306:860–866.
29. Yang, H., C.H. Lin, G. Ma, M. Orr, M.O. Baffi, and M.G. Wathelet. 2002. Transcriptional activity of interferon regulatory factor (IRF)-3 depends on multiple protein-protein interactions. *Eur. J. Biochem.* 269:6142–6151.
30. O'Connell, R.M., S.K. Saha, S.A. Vaidya, K.W. Bruhn, G.A. Miranda, B. Zarnegar, A.K. Perry, B.O. Nguyen, T.F. Lane, T. Taniguchi, et al. 2004. Type I interferon production enhances susceptibility to *Listeria monocytogenes* infection. *J. Exp. Med.* 200:437–445.
31. Stockinger, S., T. Materna, D. Stoiber, L. Bayr, R. Steinborn, T. Kolbe, H. Unger, T. Chakraborty, D.E. Levy, M. Muller, and T. Decker. 2002. Production of type I IFN sensitizes macrophages to cell death induced by *Listeria monocytogenes*. *J. Immunol.* 169:6522–6529.
32. Mattei, F., G. Schiavoni, F. Belardelli, and D.F. Tough. 2001. IL-15 is expressed by dendritic cells in response to type I IFN, double-stranded RNA, or lipopolysaccharide and promotes dendritic cell activation. *J. Immunol.* 167:1179–1187.
33. Theofilopoulos, A.N., R. Baccala, B. Beutler, and D.H. Kono. 2005. Type I interferons (alpha/beta) in immunity and autoimmunity. *Annu. Rev. Immunol.* 23:307–336.
34. Hafler, D.A. 2004. Multiple sclerosis. *J. Clin. Invest.* 113:788–794.
35. Teige, I., A. Treschow, A. Teige, R. Mattsson, V. Navikas, T. Leanderson, R. Holmdahl, and S. Issazadeh-Navikas. 2003. IFN-beta gene deletion leads to augmented and chronic demyelinating experimental autoimmune encephalomyelitis. *J. Immunol.* 170: 4776–4784.
36. Touil, T., D. Fitzgerald, G.X. Zhang, A. Rostami, and B. Gran. 2006. Cutting Edge: TLR3 stimulation suppresses experimental autoimmune encephalomyelitis by inducing endogenous IFN-beta. *J. Immunol.* 177: 7505–7509.
37. Otterbein, L.E., M.P. Soares, K. Yamashita, and F.H. Bach. 2003. Heme oxygenase-1: unleashing the protective properties of heme. *Trends Immunol.* 24:449–455.
38. Platt, J.L., and K.A. Nath. 1998. Heme oxygenase: protective gene or Trojan horse. *Nat. Med.* 4:1364–1365.
39. Beutler, B., D. Greenwald, J.D. Hulmes, M. Chang, Y.C. Pan, J. Mathison, R. Ulevitch, and A. Cerami. 1985. Identity of tumour necrosis factor and the macrophage-secreted factor cachectin. *Nature.* 316:552–554.
40. Gerard, C., C. Bruyns, A. Marchant, D. Abramowicz, P. Vandenabeele, A. Delvaux, W. Fiers, M. Goldman, and T. Velu. 1993. Interleukin 10 reduces the release of tumor necrosis factor and prevents lethality in experimental endotoxemia. *J. Exp. Med.* 177:547–550.
41. Minamino, T., H. Christou, C.M. Hsieh, Y. Liu, V. Dhawan, N.G. Abraham, M.A. Perrella, S.A. Mitsialis, and S. Kourembanas. 2001. Targeted expression of heme oxygenase-1 prevents the pulmonary inflammatory and vascular responses to hypoxia. *Proc. Natl. Acad. Sci. USA.* 98:8798–8803.
42. Weng, Y.H., G. Yang, S. Weiss, and P.A. Dennery. 2003. Interaction between heme oxygenase-1 and -2 proteins. *J. Biol. Chem.* 278: 50999–51005.
43. Lin, Q., S. Weis, G. Yang, Y.H. Weng, R. Helston, K. Rish, A. Smith, J. Bordner, T. Polte, F. Gaunitz, and P.A. Dennery. 2007. Heme oxygenase-1 protein localizes to the nucleus and activates transcription factors important in oxidative stress. *J. Biol. Chem.* 282:20621–20633.
44. Struhl, K. 1989. Helix-turn-helix, zinc-finger, and leucine-zipper motifs for eukaryotic transcriptional regulatory proteins. *Trends Biochem. Sci.* 14:137–140.
45. Harrington, L.E., R.D. Hatton, P.R. Mangan, H. Turner, T.L. Murphy, K.M. Murphy, and C.T. Weaver. 2005. Interleukin 17-producing CD4+ effector T cells develop via a lineage distinct from the T helper type 1 and 2 lineages. *Nat. Immunol.* 6:1123–1132.

46. Tuohy, V.K., M. Yu, L. Yin, P.M. Mathisen, J.M. Johnson, and J.A. Kawczak. 2000. Modulation of the IL-10/IL-12 cytokine circuit by interferon-beta inhibits the development of epitope spreading and disease progression in murine autoimmune encephalomyelitis. *J. Neuroimmunol.* 111:55–63.
47. Floris, S., S.R. Ruuls, A. Wierinckx, S.M. van der Pol, E. Dopp, P.H. van der Meide, C.D. Dijkstra, and H.E. De Vries. 2002. Interferon-beta directly influences monocyte infiltration into the central nervous system. *J. Neuroimmunol.* 127:69–79.
48. Xanthoulea, S., M. Pasparakis, S. Kousteni, C. Brakebusch, D. Wallach, J. Bauer, H. Lassmann, and G. Kollias. 2004. Tumor necrosis factor (TNF) receptor shedding controls thresholds of innate immune activation that balance opposing TNF functions in infectious and inflammatory diseases. *J. Exp. Med.* 200:367–376.
49. tenOever, B.R., S. Sharma, W. Zou, Q. Sun, N. Grandvaux, I. Julkunen, H. Hemmi, M. Yamamoto, S. Akira, W.C. Yeh, et al. 2004. Activation of TBK1 and IKKvarepsilon kinases by vesicular stomatitis virus infection and the role of viral ribonucleoprotein in the development of interferon antiviral immunity. *J. Virol.* 78: 10636–10649.
50. Becher, B., B.G. Durell, and R.J. Noelle. 2003. IL-23 produced by CNS-resident cells controls T cell encephalitogenicity during the effector phase of experimental autoimmune encephalomyelitis. *J. Clin. Invest.* 112:1186–1191.